RSC Advances

ROYAL SOCIETY OF CHEMISTRY

www.rsc.org/advances

Cite this: DOI: 10.1039/c0xx00000x

www.rsc.org/xxxxxx

ARTICLE TYPE

Synergistic effect of carbon fibers and carbon nanotubes on improving thermal stability and flame retardancy of polypropylene: A combination of physical network and chemical crosslinking†

Jiang Gong,[a,b] Ran Niu,[a,b] Xin Wen,[a] Hongfan Yang,[a,b] Jie Liu,[a] Xuecheng Chen,[a,c] Zhao-Yan Sun,[a] Ewa Mijowska,[c] and Tao Tang*[a]

Received (in XXX, XXX) Xth XXXXXXXXX 200X, Accepted Xth XXXXXXXXX 200X
DOI: 10.1039/b000000x

Recently, an intensive research effort has been devoted to the fabrication of polymer composites with enhanced physical and chemical properties. In this work, the combination of carbon fibers (CFs) and carbon nanotubes (CNTs) was demonstrated to show a synergistic effect on improving thermal stability and flame retardancy of polypropylene (PP). The results of morphology characterization indicated that both CFs and CNTs were well dispersed in the PP matrix. The temperature at the maximum weight loss rate of PP under air atmosphere was dramatically increased by 93.4 °C, and the peak value of heat release rate measured by cone calorimeter was significantly reduced by 71.7%. The remarkably improved thermal stability and flame retardancy of PP were partially owing to the accelerated oxidation crosslinking reaction of PP radicals by CNTs (chemical effect), and partially to the *in situ* formation of dense and continuous CF/CNT hybrid protective layer (physical effect). This was because the CF/CNT hybrid protective layer not only hindered the diffusion of oxygen into PP and the migration of volatile decomposition products out of PP, but also acted as a thermal shield for energy feedback from the flame.

1. Introduction

Nowadays, polypropylene (PP) has been widely used in many fields such as electronic and electric industry, automobile and housing due to its good mechanical properties, excellent electrical resistance, low toxicity, low density and good chemical resistance. However, one of the main drawbacks of PP is its inherent flammability, which restricts its application in many fields for safety consideration. Consequently, the improvement of flame retardancy of PP is not only necessary but also urgent.[1–7] Among various methods for improving flame retardancy of polymer, forming carbonaceous protective layer during combustion has been proven to be an effective method. A common way is to add intumescent flame retardant,[8,9] which typically consists of three components, namely, an acid source, a carbon source and a blowing source. The carbonaceous protective layer results from the carbonization of the added carbon source. Recently, different forms of fillers which are significantly varied in the size (nano, micro or millimeter), geometry (spherical, rod and layered) and structural properties have been widely applied as flame retardant additives to improve the flame retardancy of polymer.[10–20] The most dominant mechanism is that the formation of a network-like filler structure within polymer matrix significantly reduces the flammability of polymer,[21,22] because the continuous network-like protective layer from fillers acts as a thermal shield of energy feedback from the flame.

With the research for the utility of different fillers in composites and the demand for high performance composites, the combination of different fillers to fabricate multicomponent polymer composites with enhanced physical and chemical properties has attracted a wide of academic and industrial interests.[23–33] Song *et al.* reported the improvements of flame retardancy of PP by C60-decorated carbon nanotubes (CNTs) due to the free radical trapping effect of C60 and the network of CNTs.[34] Jose *et al.* showed that the alumina–clay nanoscale hybrid improved the mechanical and thermal properties of PP.[35] Liu *et al.* prepared the ternary polyurethane/graphene nanoribbon/CNTs composite with excellent mechanical properties and high electrical conductivity.[36] Wang *et al.* demonstrated the synergistic effect of graphene/Ni–Fe layered double hydroxide (LDH) hybrid on improving the flame retardancy of epoxy resin, which was owing to the adsorption and barrier effect of graphene and the thermal oxidative resistance of the char layer improved by Ni–Fe LDH.[37] Our group prepared many multicomponent polymer composites containing nickel particles and reactive fillers to improve the thermal stability, flame retardancy and mechanical properties of polymer.[38–46]

Despite of these efforts, the combination of macroscale carbon fibers (CFs) with nanofillers has attracted special attention because of their advantages such as light mass, high conductivity and superior reinforced-effect for polymer matrix.[47–49] The resultant CF reinforced polymer composite provides an alternative to obtain light weight material with high mechanical, electrical, thermal and chemical properties. Mirzapour *et al.* found that the combination of CFs and silica improved the

mechanical, thermal stability and ablation properties of phenolic resin.[50] Moaseri *et al.* used electrophoretic deposition and pyrolysis process to fabricate CF/CNT hybrid, which considerably enhanced tensile strength and elastic modulus of epoxy resin.[51] Puch *et al.* showed the improvements of Young's modulus and tensile strength of Nylon 6 by increasing total volume contents of CFs and CNTs.[52] Liao *et al.* proved that functional CNTs enhanced the mechanical properties of CF/vinyl ester (VE) composite by providing strong interfacial interaction between CNTs and VE matrix for improving the stress transfer from VE matrix to CFs.[53]

However, as can be seen, most of studies are limited to mechanical properties, and little attention has been paid to improving the flame retardancy. The combustion process of polymer is complicated, which takes place at least in three interdependent phases, namely, condensed phase, gas phase, and interphase. From the viewpoint of reaction, it can be simply thought to involve the breakdown of polymer chains to form macroradicals and H•, which in turn speed up the degradation of the polymer. As one of the most promising nanofillers to manufacture high performance polymer composites,[54–57] CNTs have recently been found to reduce the flammability of PP by trapping free radicals and *in situ* forming a gelled ball crosslinking network in the condensed phase.[41] Accordingly, it is possible to improve the flame retardancy of PP/CF composite by incorporating CNTs. Besides, compared to other commonly used fillers such as graphene and LDH, CFs and CNTs show advantages such as easier ability to be well dispersed in polymer matrix due to their low effective contact areas and weak interactions. More importantly, to the best of our knowledge, the synergistic effect of CFs and CNTs on improving flame retardancy of polymer has not yet been reported.

On the other hand, as described earlier, the *in situ* formation of the continuous network-like protective layer from fillers is extremely important for polymer composites to enhance the flame retardancy. This is because the continuous network-like protective layer from fillers not only prevents the diffusion of oxygen into the matrix and hinders the migration of volatile decomposition products out of matrix during thermal degradation, but only acts as a thermal shield for energy feedback from the flame. Li *et al.* reported the addition of CNTs into polyethersulfone/CF composite to improve the flame retardancy. Unfortunately, the combined CF/CNT fillers did not form a dense and compact char layer; as a result, the flame retardancy of polyethersulfone did not be improved obviously.[58] Therefore, the design and fabrication of dense and compact CF/CNT hybrid are of great significance to improve the flame retardancy of polymer.

Herein, based on the work of Kashiwagi,[21] our work is inspired by the structure of the reinforced concrete slab as shown in Fig. 1a. The long and straight rebar (Fig. 1b, just like long CFs) acts as framework, while the concrete (just like short CNTs) connects the rebar and strengthens the structure. As a result, the reinforced concrete slab shows characteristics of light weight and high strength. So, what will happen by adding CFs into polymer/CNT composite? Can CFs favor the formation of a better char layer to further improve the flame retardancy of polymer/CNT composite? In this work, the combination of CFs and CNTs was applied and demonstrated to show a synergistic effect on significantly improving flame retardancy and thermal stability of PP. The *in situ* formation of dense and compact CF/CNT hybrid (Fig. 1c, just like the reinforced concrete slab) during combustion acted as a thermal insulation layer and a barrier for evolved degradation products to the gas phase. Besides, CFs (Fig. 1d) promoted the dispersion of CNTs in PP matrix, which accelerated the oxidation crosslinking reaction of PP radicals. To the best of our knowledge, this is the first report to demonstrate the synergistic effect of CFs and CNTs on improving flame retardancy and thermal stability of polymer.

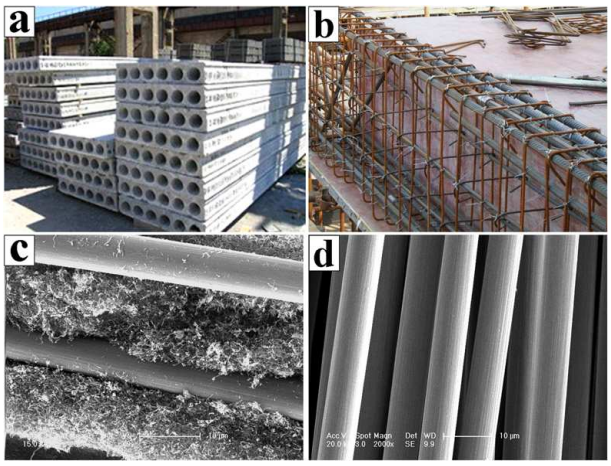

Fig. 1 Photographs of the reinforced concrete slab (a), its structure without concrete (b), and field-emission scanning electron microscope (FE-SEM) images of the *in situ* formed CF/CNT hybrid (c) and CFs (d).

2. Experiment part

2.1 Materials

Polypropylene (PP, trademark T30S, molten flow index = 6.8 g/10 min at the temperature of 230 °C under pressure of 2.16 kg, weight-average molecular weight = 28.9×10^4 g/mol, polydispersity = 3.45, and melting point = 165.5 °C) powder was supplied by Daqing Petrochemical Co., Ltd, China. The maleic anhydride grafted PP (PPMA, molten flow index = 32 g/min at the temperature of 230 °C under pressure of 2.16 kg) with 0.8 wt % of maleic anhydride group was supplied by Starbetter (Beijing) Chemical Materials Co., China. CFs with an average length of 3 mm were purchased from Shanghai Yingjia Special Fiber Material Co., China. Multi-walled CNTs with a purity of more than 98% (the main metal impurities are nickel (0.86 wt %) and iron (0.04 wt %), a diameter of 15 ± 5 nm and a length of about 30 μm were purchased from Chengdu Institute of Organic Chemistry. CNTs were ball milled at 400 rpm for 45 min before being used, and the length of CNTs was reduced to 1–3 μm according to morphology characterization.

2.2 Preparation of PP composite

PP composite was prepared by mixing PP powder, PPMA (10 wt %), CFs (5 wt %) and CNTs (5 wt %) in a Haake batch intensive mixer (Haake Rheomix 600, Karlsruhe, Germany) at 100 rpm and 180 °C for 10 min. The resultant sample was designated as 5CF5CNT. For comparison, PP with 10 wt % PPMA (simplified as PP), 10CF and 10CNT were also prepared.

The content of CFs or CNTs was selected according to the previous work.[21,22,42]

2.3 Characterization

The dispersion states of CFs and CNTs in PP matrix were examined with FE-SEM (XL30 ESEM-FEG). The samples were fractured in liquid nitrogen, and the fractured surfaces were coated with gold before FE-SEM observation. Thermal gravimetric analysis (TGA) was performed on a SDTQ600 thermal analyzer (TA Instruments). The samples for PP and its composites with mass of 7.5 ± 0.2 mg were heated from room temperature at 10 °C/min under air atmosphere. Cone calorimeter tests were performed using a Fire Testing Technology Ltd. (West Sussex, UK) device according to ISO 5660 at an incident flux of 50 kW/m^2. The samples were hot pressed by compression molding at 180 ^{o}C with the size of 100 × 100 × 6 mm square plaques. Each sample was mounted in aluminum foil and placed on a holder filled with a mineral fiber blanket, so that only the upper face was exposed to the radiant heater. All the samples were burned in triplicate, and the data were the average of three replicated tests. The photographs of the residual chars after cone calorimeter tests were collected by a digital camera. The interior structure of the residual chars was examined by FE-SEM (XL30 ESEM-FEG). The limiting oxygen index (LOI) values were measured on an HC-2C oxygen index meter (Jingning Analysis Instrument Company, China) with sheet dimensions of 130 mm × 6.5 mm × 3.2 mm according to ISO4589-1999. The samples were hot pressed by compression molding at 180 ^{o}C with the size of 130 mm × 6.5 mm × 3 mm rectangle plaques. All the samples were tested in fivefold, and the data were the average of five replicated tests. The rheological measurements of PP and its composites were carried out on a controlled strain rate rheometer (ARES rheometer). The size of samples measured was 25 mm in diameter, with a gap of 1.0 mm. Frequency sweeping was performed at 180 °C at a frequency from 0.01 to 100 rad/s in nitrogen environment, with a strain of 1% in order to make the materials be in the linear viscosity range. Temperature scanning test was performed in the range from 180 to 350 °C after samples were preheated at 180 °C for 10 min, with a strain of 1% and a fixed frequency of 0.1 rad/s in air environment. Before the measurement of gel content, PP and its composites were compressed into a film with a thickness of 0.1–0.01 mm, and then heated at 360 ^{o}C for 15 min in a muffle according to a previous reference.[3,22] The gel content was measured using a Soxhlet extractor by refluxing the samples in boiling xylene at 140 ^{o}C for 24 h, and subsequently drying in a vacuum oven at 80 ^{o}C for 24 h. The gel content was calculated by dividing the remaining mass by the original mass of the samples. Infrared spectra were recorded with a Bruker Vertex 70 FTIR spectrometer; 64 scans were collected with spectral resolution 2 cm^{-1}. Original CNTs, CFs and the residues from PP composites after Soxhlet extraction were mixed with KBr in the proportion 0.5–1 wt %, and compressed to a thin disk for analysis, respectively. Neat PP was thermal-pressed into a thin film, and then subjected to FTIR measurements under the same testing conditions as original CNTs.

3. Results and discussion

3.1 Dispersion of CFs and CNTs in PP matrix

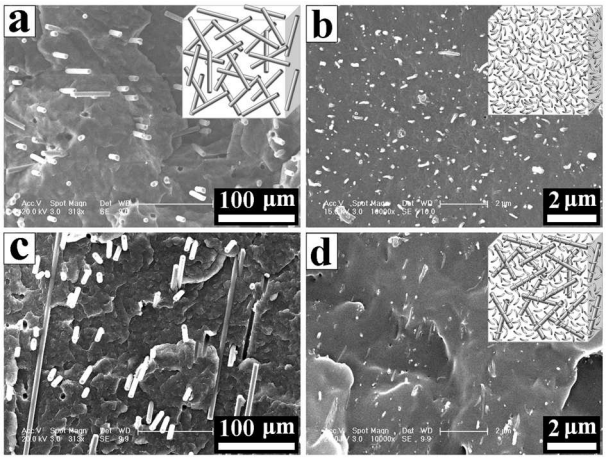

Fig. 2 Typical FE-SEM micrographs of the brittle-fractured surfaces of PP composites: 10CF (a), 10CNT (b), and 5CF5CNT (c and d). The insetting images in (a), (b) and (d) showed the schematic descriptions of 10CF, 10CNT, and 5CF5CNT, respectively.

Fig. 2 presents the dispersion states of CFs and CNTs in the PP matrix. The dispersion of fillers in polymer matrix is one of most important factors influencing the properties of polymer composites. As can be seen, the CF sticks in the binary 10CF composite were uniformly distributed (Fig. 2a). The surface of pulled-out CFs was relatively smooth and some cavities were visible. Nevertheless, the three dimensional CF structure was formed in the PP matrix as depicted in the insetting image of Fig. 2a. In the case of binary 10CNT composite, a large number of short CNTs were homogeneously distributed throughout PP matrix with few aggregates (Fig. 2b). A similar phenomenon was observed in PP/CNT/Ni_2O_3 composite from our recent study.[42] Furthermore, it was found that CNTs were adhered firmly to the PP matrix, indicating a strong interfacial interaction between CNTs and PP chains. This is ascribed to the compatibilization of PPMA, which helps to improve the dispersion of filler and the matrix-filler interaction. Similar result was found by Song *et al.*[7] As displayed in Figs. 2c and 2d, both CFs and CNTs were well dispersed without orientation (Figs. S1 and S2 in ESI†) in ternary 5CF5CNT composite and formed the composite as shown in the insetting image of Fig. 2d.

3.2 Thermal stability

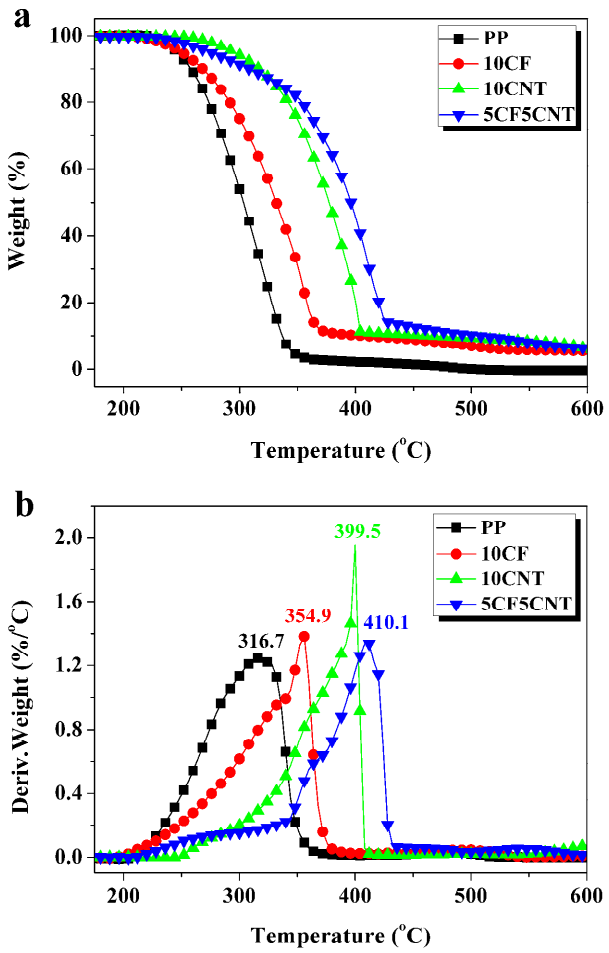

Fig. 3 TGA (a) and DTG (b) curves of PP and its composites under air atmosphere at 10 °C/min.

Table 1 Summary of the TGA results (Fig. 3) for PP and its composites.

Sample	$T_{10wt\%}$ [a] (°C)	$T_{50wt\%}$ [b] (°C)	T_{max} [c] (°C)
PP	258.0	303.4	316.7
10CF	268.3	331.7	354.9
10CNT	316.8	377.2	399.5
5CF5CNT	308.4	396.1	410.1

[a] $T_{10wt\%}$ represented the temperature at which 10 wt % weight loss occurred. [b] $T_{50wt\%}$ represented the temperature at which 50 wt % weight loss occurred. [c] T_{max} represented the temperature at which the maximum weight loss rate occurred.

To study the influences of CFs and CNTs on the thermal stability of PP, TGA measurement was conducted. Fig. 3 shows TGA and the derivative TGA (DTG) curves for PP and its composites under air atmosphere at 10 °C/min. $T_{10wt\%}$, $T_{50wt\%}$ and T_{max} represented the temperature at which 10 wt %, 50 wt % and the maximum weight loss rate occurred, respectively. The detailed data are summarized in Table 1. It was apparent that the thermal stability of all the PP composites increased compared with those of neat PP. In the case of binary 10CF composite, $T_{10wt\%}$, $T_{50wt\%}$ and T_{max} were increased by 10.3, 28.3 and 38.2 °C, respectively, compared to neat PP, indicating that CFs improved the thermal stability of PP to an extent. Comparatively, $T_{10wt\%}$, $T_{50wt\%}$ and T_{max} of binary 10CNT composite were significantly improved by 58.8, 73.8 and 82.8 °C, respectively. Interestingly, the combination of CFs with CNTs further enhanced the thermal stability of PP. $T_{10wt\%}$, $T_{50wt\%}$ and T_{max} of 5CF5CNT were raised by 50.4, 92.7 and 93.4 °C, respectively, compared to those of neat PP. That is to say, despite of slightly lower $T_{10wt\%}$ of 5CF5CNT, $T_{50wt\%}$ and T_{max} were 18.9 and 9.6 °C higher than those of 10CNT, respectively. Thereby, the combination of CFs with CNTs was more efficient than CFs or CNTs in enhancing the thermal stability of PP.

Table 2 Combustion parameters obtained from cone calorimeter and LOI tests.

Sample	t_i (s)	PHRR (kW/m^2)	THR (MJ/m^2)	Average MLR (g/s)	Residue[a] (wt %)	PSPR (m^2/s)	TSP (m^2)	PCO2P (g/s)	PCOP (g/s)	LOI (%)
PP	38±4	1284±35	214±4	0.071±0.003	1.2±0.1	0.126±0.009	50.8±1.7	0.741±0.015	0.0121±0.0008	18.2±0.2
10CF	30±2	915±26	207±3	0.054±0.002	8.8±0.7	0.358±0.021	56.1±2.0	0.555±0.010	0.0084±0.0006	20.6±0.2
10CNT	25±2	367±18	199±2	0.040±0.002	12.4±1.0	0.065±0.005	27.9±0.8	0.215±0.008	0.0029±0.0001	24.6±0.2
5CF5CNT	25±2	364±15	194±2	0.039±0.002	14.4±1.1	0.055±0.003	27.2±0.6	0.205±0.005	0.0027±0.0001	25.8±0.2

[a] Mass percentage left after testing finished.

3.3 Flammability properties

The influences of CFs and CNTs on the flame retardancy of PP were investigated by means of cone calorimetry. Cone calorimetry is one of the most effective small-sized polymer fire behavior tests. It provides important information about fire risk *via* parameters such as the time to ignition (t_i), heat release rate (HRR), peak heat release rate (PHRR), total heat release (THR), mass loss rate (MLR) and smoke production rate (SPR). The results are shown in Figs. 4–6 and Table 2. Fig. 4a shows the HRR plots of PP and its composites. Neat PP burnt very fast after ignition and a sharp HRR peak appeared with a PHRR as high as 1284 kW/m^2. The PHRR in the HRR plot (915 kW/m^2) and t_i of

binary 10CF composite changed slightly compared to those of neat PP, indicating that the flammability of PP was not influenced strongly by adding CFs alone. However, the PHRR of binary 10CNT composite (367 kW/m^2) was reduced by 71.4% compared to that of neat PP, suggesting that the flammability of PP could be reduced by adding CNTs. The lower t_i of binary 10CNT composite compared to neat PP (Table 2) was attributed to the increased thermal absorbance of PP composites by introducing CNTs. When the combination of 5 wt % CFs and 5 wt % CNTs was applied, the PHRR from the HRR plot of ternary 5CF5CNT composite (364 kW/m^2) showed a slight reduction comparing with that of binary 10CNT composite. It was worthy to note that the HRR plot of ternary 5CF5CNT composite reduced further after the peak, and stayed at a very low level throughout. Similar with 10CNT, 5CF5CNT showed lower t_i value than neat PP. Fig. 4b presents the THR curves for PP and its composites. Compared to neat PP, the THR of binary or ternary PP composites showed no obvious decreases. However, since the slope of THR curve was assumed as representing the fire spread rate,[46] the flame spread of ternary 5CF5CNT composite decreased significantly in comparison with neat PP.

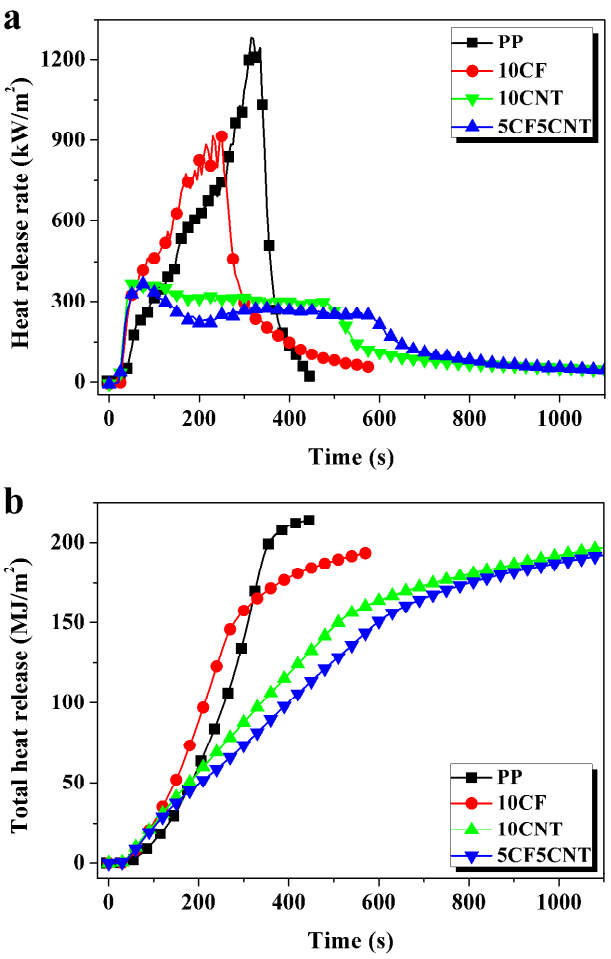

Fig. 4 Effects of CFs and CNTs on the heat release rate (a) and total heat release (b) of PP.

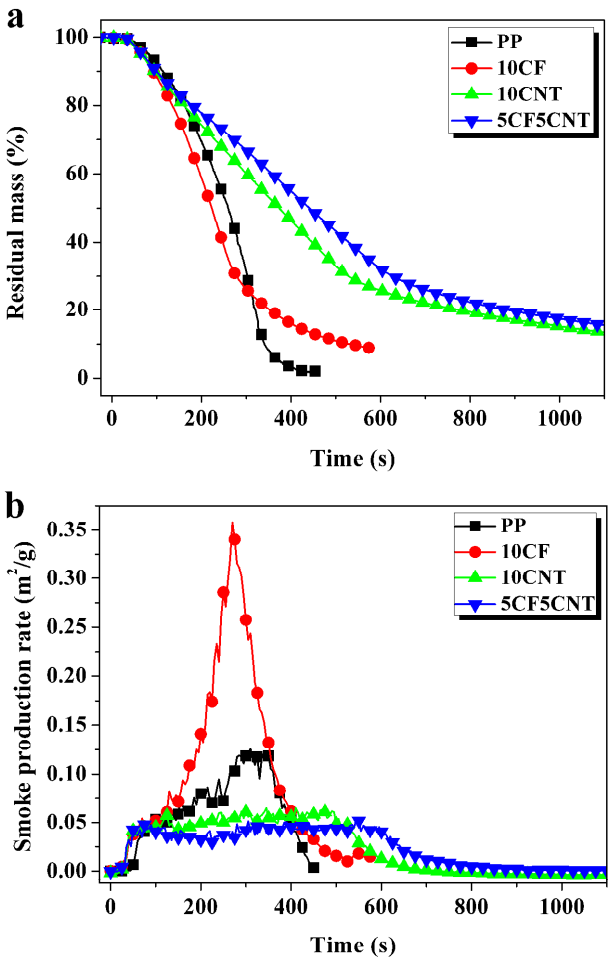

Fig. 5 Effects of CFs and CNTs on the normalized mass loss (a) and smoke production rate (b) of PP.

The mass loss rate of a polymer during combustion is very important to evaluate the flammability property. Fig. 5a shows the changes of normalized mass loss of PP and its composites with combustion time. Addition of CFs alone into PP matrix did not notably decrease the MLR, while adding CNTs alone into PP matrix led to a dramatic reduction of the MLR in the later stage of combustion. However, the combination of CFs with CNTs into PP resulted in a more dramatic increase in the residual mass during combustion for more than 450 s compared to binary 10CNT composite, meanwhile 5CF5CNT showed lower average MLR. Besides, the highest yield of residual chars for PP composites (Table 2) was 14.4 wt % from ternary 5CF5CNT composite, a little higher than the initial total loadings of CFs and CNTs. This meant that a part of pyrolytic flammable gases did not quickly volatilize during combustion in the case of ternary 5CF5CNT composite.

Smoke in a real fire means more risk of suffocation, even more fatal than heat release. Fig. 5b displays the SPR plots of PP and its composites with combustion time. The increased SPR of binary 10CF composite compared to that of neat PP was probably ascribed to CFs promoting the aromatization of PP degradation products, while after adding CNTs, the SPR decreased obviously. Besides, for the ternary 5CF5CNT composite, the SPR decreased further to a very low level. As a result, the peak SPR (PSPR) and total smoke production (TSP) were reduced from 0.126 to 0.055

m^2/s (by 56.3%) and from 50.8 to 27.2 m^2 (by 46.5%), respectively. All of the results proved that the combination of CFs and CNTs suppressed the formation of smoke very well, which is advantageous in reducing fire risk.

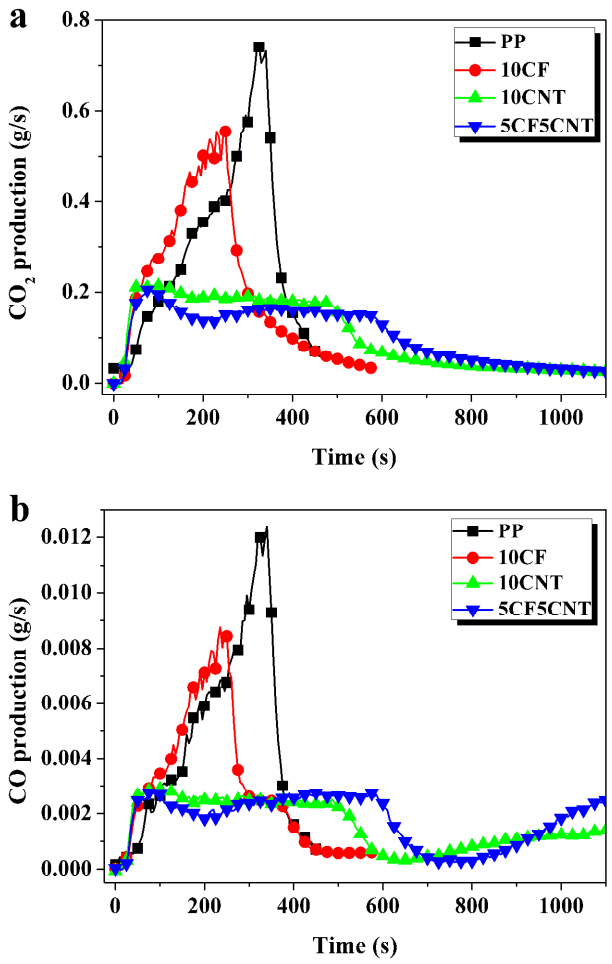

Fig. 6 Effects of CFs and CNTs on the CO_2 production (a) and CO production (b) of PP.

Fig. 6 shows the CO_2 production and CO production curves for PP and its composites. It was clear that both CFs and CNTs decreased both CO_2 production and CO production. The peak of CO_2 production (PCO2P) decreased from 0.741 g/s for neat PP to 0.555 g/s for 10CF, 0.215 g/s for 10CNT, but 0.205 g/s (by 72.3%) for 5CF5CNT. Likewise, the peak of CO production (PCOP) decreased from 0.0121 g/s for neat PP to 0.0084 g/s for 10CF, 0.0029 g/s for 10CNT, but 0.0027 g/s (by 77.7%) for 5CF5CNT. To further investigate the flame retardancy of PP composites, LOI tests were carried out. As listed in Table 2, the LOI value increased from 18.2 for PP to 20.6 or 24.6 with the incorporation of 10 wt % CFs or 10 wt % CNTs. The highest value could reach to 25.8 corresponding to ternary 5CF5CNT composite. Based on the above results, the combination of CFs with CNTs was demonstrated to show a synergistic effect on enhancing the flame retardancy of PP.

To study the synergistic effect of CFs with CNTs on improving the flame retardancy of PP, the structures of the residual chars after cone calorimeter tests were analyzed. Fig. 7 presents the photographs of the residual chars from PP and its composites. There was no any char left for neat PP after combustion at 700 °C (Fig. 7a), because of its inherent flammability with whole aliphatic hydrocarbon structure. In the case of binary 10CF composite, some blotch-like residual char was left (Fig. 7b), while a few black solids were found from binary 10CNT composite, and the char layer was not continuous (Fig. 7c). However, as shown in Fig. 7d, the char layer from ternary 5CF5CNT composite became dense, thick and fully covered, compared to that from binary 10CF or 10CNT composite. That is to say, the combination of CFs and CNTs improved the quality of char layer.

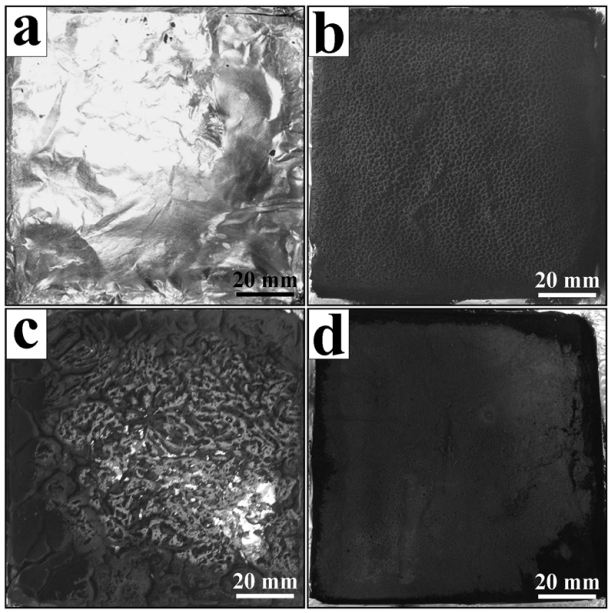

Fig. 7 Photographs of the residual chars after cone calorimeter tests: neat PP (a), 10CF (b), 10CNT (c) and 5CF5CNT (d).

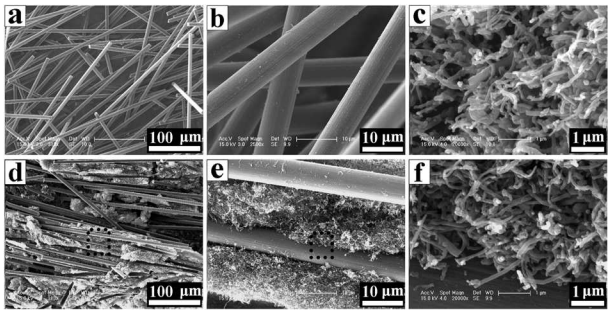

Fig. 8 FE-SEM micrographs of the residual chars after cone calorimeter tests: 10CF (a and b), 10CNT (c) and 5CF5CNT (d–f).

The interior structure of residual chars was observed by FE-SEM. As depicted in Fig. 8a, the residual char from binary 10CF composite consisted of many individual CF sticks with little carbon remained on the surface (Fig. 8b). The residual char from binary 10CNT composite was composed of short winding CNTs (Fig. 8c). A lot of CF sticks with block-like carbon were observed

in the residual char from ternary 5CF5CNT composite, but more residual carbon were adhered onto the surface of CFs (Figs. 8d–8f). Particularly, many CF sticks were inserted in the block-like carbon, demonstrating the formation of integrated and continuous three dimensional CF/CNT hybrid structure (just like the reinforced concrete slab as shown in Fig. 1a) in the residual char from 5CF5CNT during combustion. In other words, the combination of CFs with CNTs promoted the formation of a better dense and continuous carbon protective layer than CFs or CNTs alone. The carbon layer enhanced the physical barrier effect, which not only prevented the diffusion of oxygen into PP matrix, but also hindered the migration of volatile decomposition products out of PP. Additionally, the carbon layer acted as a thermal shield for energy feedback from the flame during combustion. Consequently, the improved char layer was contributed to the synergistic effect of CFs and CNTs on improving the flame retardancy of PP.

3.4 Combined CF/CNT forming a network structure in PP matrix

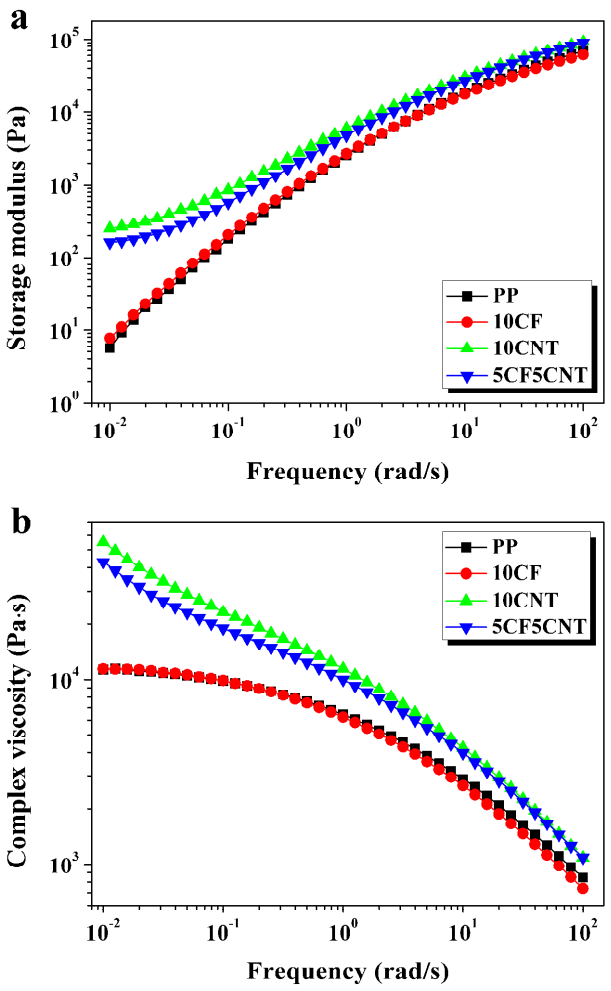

Fig. 9 Effects of CFs and CNTs on linear viscoelastic properties: Storage modulus (a) and complex viscosity (b).

To study whether the combination of CFs with CNTs formed a percolated network structure in PP matrix, melt rheological properties of PP and its composites were investigated. Fig. 9a shows the variations of storage modulus (G') and complex viscosity (η) as a function of frequency (ω) for neat PP and its composites at 180 °C under nitrogen atmosphere. Neat PP exhibited a typical linear polymer-like terminal behavior with scaling properties of approximately $G' \sim \omega^2$, indicating that PP molecular chains were fully relaxed at low frequencies. When 10 wt % CFs were added, there were no plateau at the low frequencies, implying that the content of CFs did not reach the threshold values to form the network. However, this terminal behavior was significantly changed when 10 wt % CNTs were incorporated into PP matrix, and the dependence of G' on ω at low frequencies became weak. For ternary 5CF5CNT composite, the G' curve exhibited a distinct plateau at the low frequencies. Similar phenomena were observed in polystyrene/CNTs and polystyrene/clay,[1] PP/CNTs[59] and PP/graphene/fumed silica.[60] The above results demonstrated a transition from liquid-like to solid-like viscoelastic behavior in ternary 5CF5CNT composite.

It is well known that the melting process and degradation will take place before a material starts to combust, and combustible gas products will traverse the decomposition zone to the flame zone to maintain combustion. If the melt viscosity is high, the gas products need more time to reach the flame zone, and the combustion process will thus be slowed down. Correspondingly, the change of η for PP and its composites is shown in Fig. 9b. Neat PP displayed a pseudo-Newtonian behavior at low frequency range, and this behavior did not change significantly with the addition of 10 wt % CFs. Interestingly, in the binary 10CNT and ternary 5CNT5CF composites, a much higher complex viscosity and a pronounced shear thinning behavior were present. This behavior confirmed that the combination of CFs with CNTs promoted the formation of percolated network, which was essential to improve the char layer and the flame retardancy of PP.

3.5 Combined CF/CNT promoting the oxidation crosslinking reaction of PP

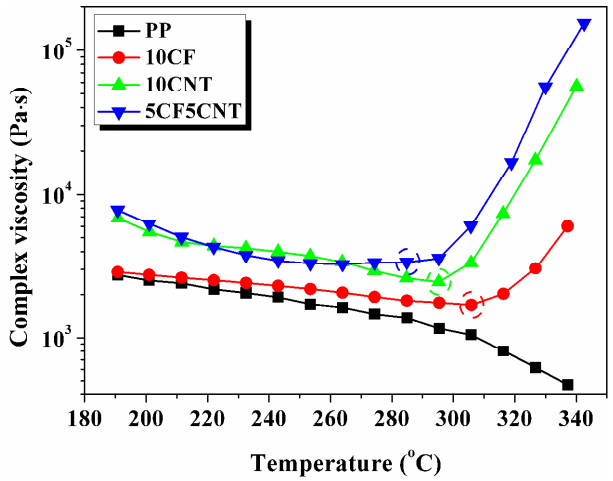

Fig. 10 Dependence of complex viscosity on temperature for PP and its composites under air atmosphere. The cycled data point displayed the onset temperature for complex viscosity increase of PP composites.

Generally, the degradation of PP is a free radical chain reaction

through β-scission of polymer chains, and the degradation will speed up in the presence of O_2. Thus, it was possible that the CF/CNT hybrid promoted the thermal-oxidative crosslinking degradation reaction of PP, which made a positive contribution to the thermal stability and flame retardancy. To confirm this speculation, dynamic temperature scanning measurements were performed on the neat PP and its composites under air atmosphere. Fig. 10 presents the curves of temperature dependence of complex viscosity for PP and its composites. All of the PP composites firstly showed a decrease in the complex viscosity with the increase of temperature, followed by a subsequent sharp increase, while a continuous decrease throughout to nearly zero was observed for neat PP. This behavior could be explained as follows: Upon heating, the easier movement of PP chains and the degradation at high temperature resulted in a decrease in complex viscosity of the samples. The increase of complex viscosity in PP composites was owing to fillers acting as oxidation crosslinking sites and the oxidation crosslinking reaction overwhelming the PP decomposition. In the case of binary 10CF composite, the temperature at which the complex viscosity began to increase was around 306 °C, implying a positive effect on restricting the oxidation degradation of PP chains, while that for binary 10CNT composite decreased down to 295 °C. This was ascribed to the quenching free radicals effect of CNTs due to their high electron affinity with sp^2 bond architecture. Comparatively, the ternary 5CF5CNT composite showed the onset temperature for complex viscosity increase at 285 °C, much lower than that of binary 10CF or 10CNT composite, which demonstrated the synergistic effect of CFs with CNTs on accelerating oxidation crosslinking reaction of PP radicals. This was probably ascribed to CFs promoting the dispersion of CNTs in PP matrix (Fig. 2), resulting from the interaction between CFs and CNTs, which decreased the interaction of dispersed CNTs to an extent (preventing re-aggregation), and the milling media role of CFs to break up CNT agglomerates during mixing.

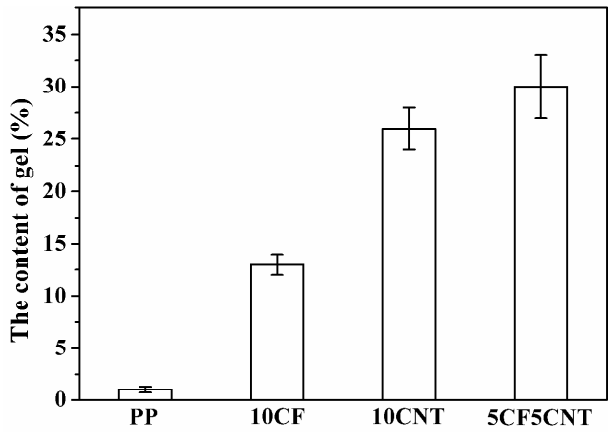

Fig. 11 The content of gel from PP and its composites after heat treatment at 360 °C for 15 min.

In order to verify the oxidation crosslinking reaction, the gel content of PP and its composites was determined. Fig. 11 presents the gel content of neat PP and its composites after heat treatment. The gel content of neat PP was very low, indicating no obvious thermal oxidation crosslinking reaction. In comparison, the gel content of PP composites was much higher than that of neat PP, and 5CF5CNT showed the highest gel content. The above results provided the evidence of the oxidation crosslinking reaction between PP and CNT/CF.

FTIR analysis also provided important evidence for the reaction. Fig. 12a shows the FTIR spectra of original CNTs, CFs, neat PP and the residues from PP composites after Soxhlet extraction. There were no apparent absorption peaks for original CNTs and CFs due to the highly absorbing nature of CNTs and CFs. Several strong bands appeared in the spectra for the residues from 10CF, 10CNT and 5CF5CNT composites. Compared to these bands with the characteristic bands of neat PP, their main peaks were good consistent with those of PP. These results proved that PP chains were grafted onto the surface of CFs and CNTs. Furthermore, new peaks at 1220 and 887 cm^{-1} appeared in the 10CF, 10CNT and 5CF5CNT composites in the amplified spectra (Fig. 12b), which did not belong to vibration modes of PP, and were assigned to the stretching vibration of C–O and O–O of C–O–O–C.[22] This further proved the oxidation crosslinking reaction between PP and CF/CNT in the presence of O_2, which was in agreement with the rheological results (Fig. 10).

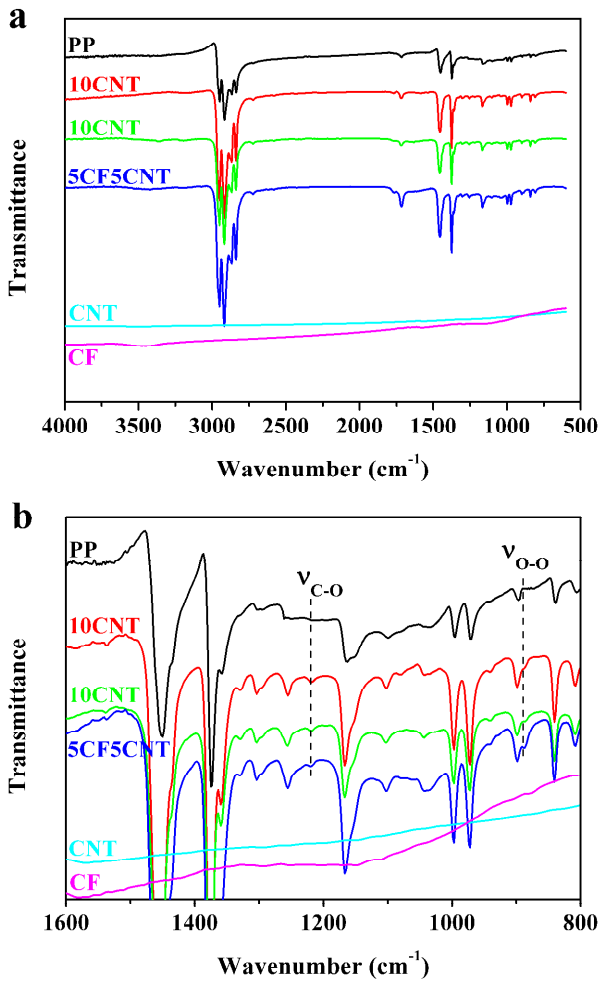

Fig. 12 FTIR spectra for original CNTs, CFs, neat PP and the residues from PP composites: (a) initial spectra between 4000 and 600 cm^{-1}; (b) magnified spectra between 1600 and 800 cm^{-1}.

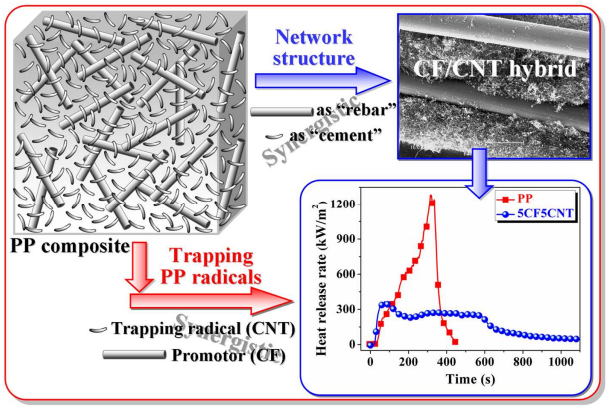

Fig. 13 Mechanism about the synergistic effect between CFs and CNTs on improving the flame retardancy of PP.

According to the above results, a schematic drawing for the mechanism of the synergistic effect between CFs and CNTs on improving the flame retardancy of PP is shown in Fig. 13. In the combination of CFs with CNTs, on one hand, a network structure of CFs and CNTs in PP matrix was formed, which facilitated the formation of a better dense and continuous CF/CNT hybrid protective layer (just like the reinforced concrete slab as shown in the Fig. 1a) in the residual char during combustion (physical effect). This not only prevented the diffusion of oxygen into PP matrix, and the migration of volatile decomposition products out of PP during thermal degradation, but also acted as a thermal shield for energy feedback from the flame. On the other hand, CFs facilitated the dispersion of CNTs in the PP matrix and contributed to trapping PP radicals by CNTs to promote the oxidation crosslinking reaction (chemical effect). Thereby, the synergistic effect of CFs and CNTs was displayed on improving the flame retardancy of PP.

Conclusions

We demonstrated the synergistic effect of CFs and CNTs on improving thermal stability and flame retardancy of PP. According to the morphology characterization of the brittle-fractured surfaces of PP composites, both CFs and CNTs were well dispersed in the PP matrix, resulting in the formation of the composite. The temperature at the maximum weight loss rate of PP under air atmosphere was dramatically increased by 93.4 ^{o}C, and the peak value of heat release rate measured by cone calorimeter was remarkably reduced by 71.7%. The significantly improved thermal stability and flame retardancy of PP were partially attributed to the *in situ* formation of the dense and continuous CF/CNT hybrid protective layer, and partially to the accelerated oxidation crosslinking reaction of PP radicals by CNTs. The dense and continuous CF/CNT hybrid protective layer prevented the diffusion of oxygen into PP and the migration of volatile decomposition products out of PP, and acted as a thermal shield for energy feedback from the flame. It is believed that this work opens up a new and exciting opportunity for fabricating hybrid to improve chemical properties (such as thermal stability and flame retardancy) of polymeric materials.

Acknowledgements

We would like to thank the reviewers for kind and important suggestions. This work was supported by the National Natural Science Foundation of China (51373171, 21204079, 51233005 and 21374114) and Polish Foundation (No. 2011/03/D/ST5/06119).

Notes and references

[a] *State Key Laboratory of Polymer Physics and Chemistry, Changchun Institute of Applied Chemistry, Chinese Academy of Sciences, Changchun 130022, China. Fax: +86 (0) 431 85262827; Tel: +86 (0) 431 85262004; E-mail: ttang@ciac.ac.cn*
[b] *University of Chinese Academy of Sciences, Beijing 100049, China*
[c] *Institute of Chemical and Environment Engineering, West Pomeranian University of Technology, Szczecinul. Pulaskiego 10, 70-322 Szczecin, Poland*
†Electronic Supplementary Information (ESI) available: Typical FE-SEM images of 5CF5CNT composite with low and high magnifications. See DOI: 10.1039/b000000x/

References

1 J. W. Gilman, C. L. Jackson, A. B. Morgan, R. Harris, E. Manias, E. P. Giannelis, M. Wuthenow, D. Hilton and S. H. Phillips, *Chem. Mater.*, 2000, **12**, 1866–1873.
2 D. D. Yang, Y. Hu, L. Song, S. B. Nie, S. Q. He and Y. B. Cai, *Polym. Degrad. Stab.*, 2008, **93**, 2014–2018.
3 P. A. Song, Y. Zhu, L. F. Tong and Z. P. Fang, *Nanotechnology*, 2008, **19**, 225707.
4 Z. B. Shao, C. Deng, Y. Tan, M. J. Chen, L. Chen and Y. Z. Wang, *ACS Appl. Mater. Interfaces*, 2014, **6**, 7363–7370.
5 T. Kashiwagi, E. Grulke, J. Hilding, K. Groth, R. Harris, K. Butler, J. Shields, S. Kharchenko and J. Douglas, *Polymer*, 2004, **45**, 4227–4239.
6 Q. L. He, T. T. Yuan, X. R. Yan, D. W. Ding, Q. Wang, Z. P. Luo, T. D. Shen, S. Y. Wei, D. P. Cao and Z. H. Guo, *Macromol. Chem. Phys.*, 2014, **215**, 327–340.
7 P. A. Song, L. H. Xu, Z. H. Guo, Y. Zhang and Z. P. Fang, *J. Mater. Chem.*, 2008, **18**, 5083–5091.
8 G. Camino, G. Martinasso and L. Costa, *Polym. Degrad. Stab.*, 1984, **7**, 25–31.
9 X. Q. Liu, D. Y. Wang, X. L. Wang, L. Chen and Y. Z. Wang, *Polym. Degrad. Stab.*, 2011, **96**, 771–777.
10 B. Schartel, P. Pötschke, U. Knoll and M. Abdel-Goa, *Eur. Polym. J.*, 2005, **41**, 1061–1070.
11 T. Kashiwagi, M. Mu, K. Winey, B. Cipriano, S. R. Raghavan, S. Pack, M. Rafailovich, Y. Yang, E. Grulke, J. Shields, R. H. Harris and J. Douglas, *Polymer*, 2008, **49**, 4358–4368.
12 S. S. Rahatekar, M. Zammarano, S. Matko, K. K. Koziol, A. H. Windle, M. Nyden, T. Kashiwagi and J. W. Gilman, *Polym. Degrad. Stab.*, 2010, **95**, 870–879.
13 S. Bourbigot, G. Fontaine, A. Gallos and S. Bellayer, *Polym. Adv. Technol.*, 2011, **22**, 30–37.
14 J. W. Gilman, C. L. Jackson, A. B. Morgan, R. H. Harris, E. Manias, E. P. Giannelis, M. Wuthernow, D. Hilton and S. H. Phillips, *Chem. Mater.*, 2000, **12**, 1866–1873.
15 S. Bourbigot, D. L. Vanderhart, J. W. Gilman, S. Bellayer, H. Stretz and D. R. Paul, *Polymer*, 2004, **45**, 7627–7638.
16 Z. Wang, X. H. Du, H. O. Yu, Z. W. Jiang, J. Liu and T. Tang, *Polymer*, 2009, **50**, 5794–5802.
17 C. Deng, J. Zhao, C. L. Deng, Q. Lv, L. Chen and Y. Z. Wang, *Polym. Degrad. Stab.*, 2014, **103**, 1–10.
18 Z. Matusinovic and C. A. Wilkie, *J. Mater. Chem.*, 2012, **22**, 18701–18704.
19 Y. S. Gao, J. W. Wu, Q. Wang, C. A. Wilkie and D. O'Hare, *J. Mater. Chem. A*, 2014, **2**, 10996–11016.
20 B. Dittrich, K. A. Wartig, D. Hofmann, R. Mülhaupt and B. Schartel, *Polym. Degrad. Stab.*, 2013, **98**, 1495–1505.

21 T. Kashiwagi, F. M. Du, J. F. Douglas, K. I. Winey, R. H. Harris, Jr and J. R. Shields, *Nat. Mater.*, 2005, **4**, 928–933.

22 X. Wen, Y. J. Wang, J. Gong, J. Liu, N. N. Tian, Y. H. Wang, Z. W. Jiang, J. Qiu and T. Tang, *Polym. Degrad. Stab.*, 2012, **97**, 793–801.

23 L. Jiang, C. Zhang, M. K. Liu, Z. Yang, W. W. Tjiu and T. X. Liu, *Compos. Sci. Technol.*, 2014, **91**, 98–103.

24 P. A. Song, Y. Shen, B. X. Du, Z. H. Guo and Z. P. Fang, *Nanoscale*, 2009, **1**, 118–121.

25 P. A. Song, L. N. Liu, S. Y. Fu, Y. M. Yu, C. D. Jin, Q. Wu, Y. Zhang and Q. Li, *Nanotechnology*, 2013, **24**, 125704.

26 W. D. Zhang, I. Y. Phang and T. X. Liu, *Adv. Mater.*, 2006, **18**, 73–77.

27 C. Zhang, W. W. Tjiu, T. X. Liu, W. Y. Lui, I. Y. Phang and W. D. Zhang, *J. Phys. Chem. B*, 2011, **115(13)**, 3392–3399.

28 Z. Wang, X. Y. Meng, J. Z. Li, X. H. Du, S. Y. Li, Z. W. Jiang and T. Tang, *J. Phys. Chem. C*, 2009, **113**, 8058–8064.

29 X. D. Qian, B. Yu, C. L. Bao, L. Song, B. B. Wang, W. Y. Xing, Y. Hu and R. K. K. Yuen, *J. Mater. Chem. A*, 2013, **1**, 9827–9836.

30 S. Liu, H. Q. Yan, Z. P. Fang, Z. H. Guo and H. Wang, *RSC Adv.*, 2014, **4**, 18652–18659.

31 H. Y. Ma, L. Tong, Z. Xu and Z. P, Fang, *Nanotechnology*, 2007, **18**, 375602.

32 K. Q. Zhou, W. Yang, G. Tang, B. B. Wang, S. H. Jiang, Y. Hu and Z. Gui, *RSC Adv.*, 2013, **3**, 25030–25040.

33 J. Gong, R. Niu, N. N. Tian, X. C. Chen, X. Wen, J. Liu, Z. Y. Sun, E. Mijowska and T. Tang, *Polymer*, 2014, **55**, 2998–3007.

34 P. A. Song, L. P. Zhao, Z. H. Cao and Z. P. Fang, *J. Mater. Chem.*, 2011, **21**, 7782–7788.

35 J. P. Jose and S. Thomas, *Phys. Chem. Chem. Phys.*, 2014, **16**, 14730–14740.

36 M. K. Liu, C. Zhang, W. W. Tjiu, Z. Yang, W. Z. Wang and T. X. Liu, *Polymer*, 2013, **54**, 3124–3130.

37 X. Wang, S. Zhou, W. Y. Xing, B. Yu, X. M. Feng, L. Song and Y. Hu, *J. Mater. Chem. A*, 2013, **1**, 4383–4390.

38 T. Tang, X. C. Chen, X. Y. Meng, H. Chen and Y. P. Ding, *Angew. Chem. Int. Ed.*, 2005, **44**, 1517–1520.

39 T. Tang, X. C. Chen, H. Chen, X. Y. Meng, Z. W. Jiang and W. G. Bi, *Chem. Mater.*, 2005, **17**, 2799–2802.

40 R. J. Song, Z. W. Jiang, H. O. Yu, J. Liu, Z. J. Zhang, Q. W. Wang and T. Tang, *Macromol. Rapid. Commun.*, 2008, **29**, 789–793.

41 H. O. Yu, Z. W. Jiang, J. W. Gilman, T. Kashiwagi, J. Liu, R. J. Song and T. Tang, *Polymer*, 2009, **50**, 6252–6258.

42 H. O. Yu, J. Liu, Z. Wang, Z. W. Jiang and T. Tang, *J. Phys. Chem. C*, 2009, **113**, 13092–13097.

43 H. O. Yu, Z. J. Zhang, Z. Wang, Z. W. Jiang, J. Liu, L. Wang, D. Wan and T. Tang, *J. Phys. Chem. C*, 2010, **114**, 13226–13233.

44 X. Wen, J. Gong, H. O. Yu, Z. Liu, D. Wan, J. Liu, Z. W. Jiang and T. Tang, *J. Mater. Chem.*, 2012, **22**, 19974–19980.

45 J. Gong, N. N. Tian, J. Liu, K. Yao, Z. W. Jiang, X. C. Chen, X. Wen, E. Mijowska and T. Tang, *Polym. Degrad. Stab.*, 2014, **99**, 18–26.

46 J. Gong, N. N. Tian, X. Wen, X. C. Chen, J. Liu, Z. W. Jiang, E. Mijowska and T. Tang, *Polym. Degrad. Stab.*, 2014, **104**, 18–27.

47 S. Y. Fu, B. Lauke, E. Mäder, C. Y. Yue and X. Hu, *Compos. Part A*, 2000, **31(10)**, 1117–1125.

48 S. Y. Fu, B. Lauke, E. Mäder, C. Y. Yue, X. Hu and Y. W. Mai, *J. Mater. Sci.*, 2001, **36(5)**, 1243–1251.

49 E. Frank, L. M. Steudle, D. Ingildeev, J. M. Spçrl and M. R. Buchmeiser, *Angew. Chem. Int. Ed.*, 2014, **53**, 5262–5298.

50 A. Mirzapour, M. H. Asadollahi, S. Baghshaei and M. Akbari, *Compos. Part A*, 2014, **63**, 159–167.

51 E. Moaseri, M. Karimi, M. Maghrebi and M. Baniadam, *Compos. Part A*, 2014, **60**, 8–14.

52 F. Puch and C. Hopmann, *Polymer*, 2014, **55**, 3015–3025.

53 W. H. Liao, H. W. Tien, S. T. Hsiao, S. M. Li, Y. S. Wang, Y. L. Huang, S. Y. Yang, C. C. M. Ma and Y. F. Wu, *ACS Appl. Mater. Interfaces*, 2013, **5**, 3975–3982.

54 J. Kim, S. M. Hong, S. Kwak and Y. Seo, *Phys. Chem. Chem. Phys.*, 2009, **11**, 10851–10859.

55 J. Liu, L. Q. Zhang, D. P. Cao and W. C. Wang, *Phys. Chem. Chem. Phys.*, 2009, **11**, 11365–11384.

56 X. L. Yan, T. Suzuki, Y. Kitahama, H. Sato, T. Itoh and Y. Ozaki, *Phys. Chem. Chem. Phys.*, 2013, **15**, 20618–20624.

57 Y. Y. Gao, J. Liu, J. X. Shen, L. Q. Zhang, Z. H. Guo and D. P. Cao, *Phys. Chem. Chem. Phys.*, 2014, **16**, 16039–16048.

58 C. Li, N. J. Kang, S. D. Labrandero, J. T. Wan, C. González and D. Y. Wang, *Ind. Eng. Chem. Res.*, 2014, **53**, 1040–1047.

59 S. B. Kharchenko, J. F. Douglas, J. Obrzut, E. A. Grulke and K. B. Migler, *Nat. Mater.*, 2004, **3(8)**, 564–568.

60 J. Gong, R. Niu, J. Liu, X. C. Chen, X. Wen, E. Mijowska, Z. Y. Sun and T. Tang, *RSC Adv.*, 2014, **4**, 33776–33784.

Table of Contents (TOC)

Synergistic effect of carbon fibers and carbon nanotubes on improving thermal stability and flame retardancy of polypropylene: A combination of physical network and chemical crosslinking

Jiang Gong, Ran Niu, Xin Wen, Hongfan Yang, Jie Liu, Xuecheng Chen, Zhao-Yan Sun, Ewa Mijowska, and Tao Tang*

CFs and CNTs showed a synergistic effect on significantly improving the thermal stability and flame retardancy of PP.